

See discussions, stats, and author profiles for this publication at: <https://www.researchgate.net/publication/367328289>

Using Obstacle Perforation, Reconfiguration, and Inclination ... THERMAL SCIENCE: Year 2022

Article · January 2023

CITATIONS

0

READS

81

8 authors, including:



Khaled Mahdi

Université de M'sila

20 PUBLICATIONS 51 CITATIONS

[SEE PROFILE](#)



Khalida Bekrentchir

Université de M'sila

5 PUBLICATIONS 3 CITATIONS

[SEE PROFILE](#)



Ahmed Kadhim Hussein

University of Babylon

215 PUBLICATIONS 5,754 CITATIONS

[SEE PROFILE](#)



Ali Akgül

Siirt Üniversitesi

605 PUBLICATIONS 7,179 CITATIONS

[SEE PROFILE](#)

USING OBSTACLE PERFORATION, RECONFIGURATION, AND INCLINATION TECHNIQUES TO ENHANCE THE DYNAMIC AND THERMAL STRUCTURE OF A TOP-ENTRY CHANNEL

by

**Khaled MAHDI^a, Khalida BEKRENTCHIR^b, Ahmed Kadhim HUSSEIN^{c,d},
Ali AKGUL^{e,f,g}, Hussein SHANAK^h, Jihad ASAD^{h*},
Nevzat AKKURTⁱ, and Younes MENN^j**

^aDepartment of Physics, University of M'sila, M'sila, Algeria

^bDepartment of Chemistry, University of M'sila, M'sila, Algeria

^cMechanical Engineering Department, College of Engineering, University of Babylon, Babylon City, Hilla, Iraq

^dCollege of Engineering, University of Warith Al-Anbiyaa, Karbala, Iraq

^eDepartment of Computer Science and Mathematics, Lebanese American University, Beirut, Lebanon

^fDepartment of Mathematics, Art and Science Faculty, Siirt University, Siirt, Turkey

^gMathematics Research Center, Department of Mathematics, Near East University, Nicosia /Mersin 10, Turkey

^hDepartment of Physics, Faculty of Applied Sciences, Palestine Technical University, Kadoorie, Tulkarm, Palestine

ⁱDepartment of Mechanical Engineering, Munzur University, Tunceli, Turkey

^jDepartment of Technology, University Center Salhi Ahmed Naama (Ctr. Univ. Naama), Naama, Algeria

Original scientific paper

<https://doi.org/10.2298/TSCI22S1475M>

This research is to incorporate three efficient ways that will increase the performance of baffled heat exchangers. The 1st technique is represented by baffle perforating to create pores through which secondary streams pass in order to reduce main stream pressure on the flow areas. A 2nd technique represented in redesigning the baffle structure by replacing its square edge with the arched edge in order to increase the X-velocity to facilitate the flow towards the outlet and reduce the Y-velocity to reduce the values of fluid friction with the solid areas. Finally, a 3rd way was demonstrated by using the inclined baffle model. Reinforcement of the baffle structure allowed for enhanced vortices, increased thermal gradients, and thus a reinforced thermodynamic structure over the entire heat exchanger.

Key words: reconfiguration, perforation, inclination, obstacle, simulation.

Introduction

Air solar exchanger channels only produce average thermal yields because of the air's poor thermophysical characteristics when utilized as a heat transfer fluid. Several methods are employed to optimize the heat exchange between the fluid and the heated surfaces. The addition of obstructions, *i.e.*, fins and baffles, to the channel's conduit is one of these

*Corresponding author, e-mail: j.asad@ptuk.edu.ps

ways. Naturally, this addition necessitates taking into account the size, shape, orientation, disposition, and number of these baffles' rows, as well as the channel's input and output shapes. These obstructions can be placed either on the upper wall or the lower surface, or by combining the two, in order to stretch the fluid's path, cause turbulence, generate recirculation, and enhance the surface area for heat exchange. As a result, heat transfer is increased, and performance is noticeably enhanced. Various studies have included simple obstacles in several heat exchanger channels [1, 2]. Moreover, the use of shaped obstacles is the goal of many recent studies [3, 4]. Both simple and modified models demonstrated improved heat transfer, but with very high friction, which results in energy loss. Others turned to a new design that included the obstacle's perforated structure to address the issue [5, 6]. In this design, the flow passes through the obstacle as the main stream while it passes through the holes as a secondary stream, relieving pressure on the high-velocity flow zones. Moreover, instead of using perforated obstacles, another model was given to the obstruction, which is the inclined baffles [7, 8], particularly in the direction of the current, which significantly reduces friction values and improves performance, tab. 1.

Table 1. Give examples of some of the research that employed various obstacle patterns


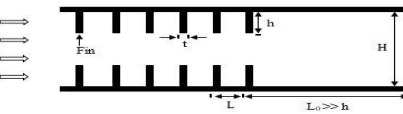

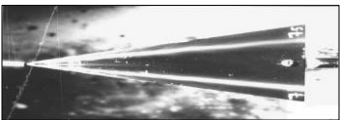
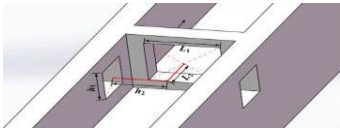


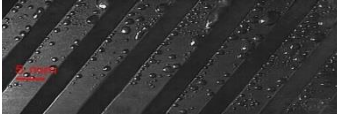
Author (s)	Physical model	Physical domain
Simple obstacles		
Berner <i>et al.</i> [1]	Flow over baffles.	
Bazdid-Tehrani <i>et al.</i> [2]	Transverse finned channel	
Shaped obstacles		
Ben Slama [3]	Flow around a baffle with a delta shape.	
Du <i>et al.</i> [4]	Segmented baffle heat exchanger.	
Perforated baffles		
Liu <i>et al.</i> [5]	Perforated walls and baffles on a micro-channel sink.	
Nakhchi <i>et al.</i> [6]	Elliptic turbulators with perforations in heat exchangers.	



Table 1. Continuation

Inclined baffles		
Yongsiri <i>et al.</i> [7]	Channels with twisted baffles running transversely and slanted.	
Yan <i>et al.</i> [8]	Inclined ribbed channels.	

In order to improve the heat transfer of a solar heat exchanger, the current study mostly uses obstacles. A reinforced obstacle design is made using three technologies. Inserting square pores on the obstacle area is the first technique. Modifying the geometry of the obstacle is the second method. Utilizing tilt geometry to take advantage of the obstacle's angle of attack constitutes the third strategy. Flow is carried out in a horizontal heat exchanger in the presence of turbulent air, with a flow rate, standing from 5000-15000, in terms of Reynolds number.

Definition of the heat exchanger used

The study's primary focus is on providing the majority of the hydrodynamic and thermal parameters of the overall performance of a heat exchanger that is baffled with various obstructions as it is shown in fig. 1(a). There is a first baffle of rectangular shape which is installed in the upper half of the exchanger, fig. 1(b). Its structure is improved through the use of two techniques simultaneously, namely, perforating and reconfiguring. The first technique is being tested by creating a pore in the center of the baffle in order to reduce the flow pressure value on the front side of the baffle. The same baffle changes its shape by curving its front upper edge in order to increase the horizontal component of velocity, *i.e.*, in order to decrease the vertical component of velocity to reduce the friction values on the opposite wall. There is a second baffle, which is fixed to the lower wall, and its geometry is also enhanced. The baffle has a top inclined at an angle of 45° with respect to the vertical axis, fig. 1(c).

On the other hand, the entrance to the canal has a height of 0.08 m and a length of 0.138 m, while the canal's conduit expands by expanding its height to 0.146 m. The following dimensions, *i.e.*, L , L_1 , L_2 , L_3 , H_2 , h , and e , were taken from the experimental study by Demartini *et al.* [9].

In the presence of air fluid, the current flows through the exchanger with a variable flow rate Reynolds number from 5000-15000. The inlet velocity is uniform [9], according to the horizontal axis, while the atmospheric pressure is taken at the outlet [9]. The channel walls are thermally insulated except for a portion of the lower wall, opposite the first baffle, extending from the left side of the exchanger to the front side of the second baffle, which is subject to a constant temperature, $T_w = 375$ K [10].

Flow is governed by the equations of conservation of mass, momentum and energy as shown in many of our previous studies [11-15]. Both the $k-\varepsilon$ model [16] and the finite-volume method [17] are used. Except for the portions close to the solid boundary, the mesh is uniform throughout the whole of the exchanger area. As for the validity of the method used, the present model utilized in the case of $S = 0.218$ m ($= L_1$) and $H_1 = 0.146$ m ($= H_2$), in the

absence of perforation, reconfiguration and inclination of baffles (it becomes a flat finned channel), can be compared with the experimental model [13]. This statement was also made in many of our previous studies [11-15].

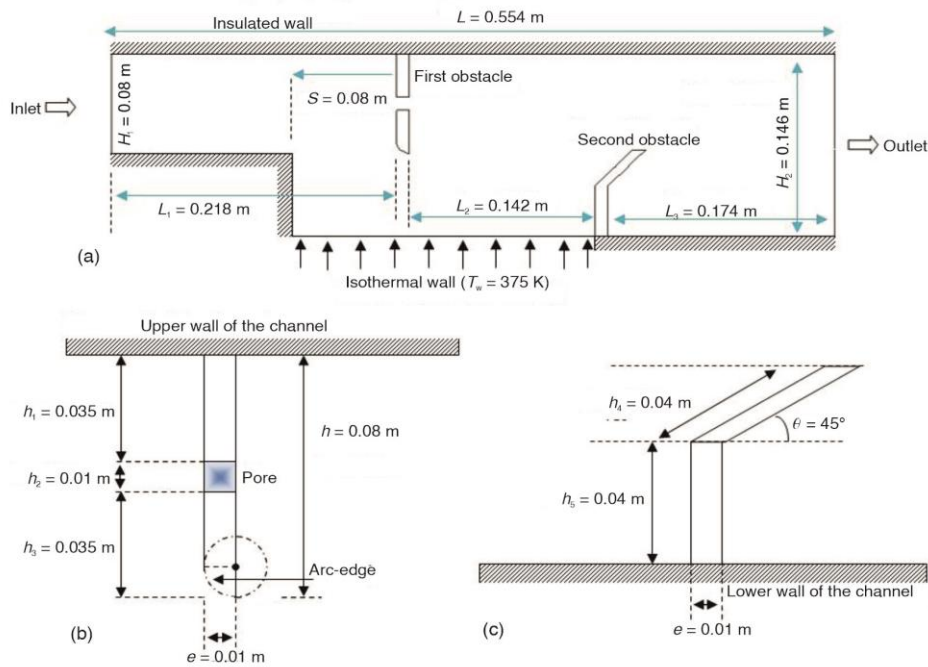


Figure 1. The studied geometrical model; (a) the baffled channel under study, (b) first baffle details, and (c) second baffle details

Results and analyzes

Regular structure of flow lines, φ , over the entire entrance due to the absence of obstructions. The flow stream widens due to the expansion in the channel height from 0.08 m to 0.146 m. The perforated obstacle, located in the upper section of the channel opposite its entrance, receives a parallel current which is changed from its direction by its left side, fig. 2.

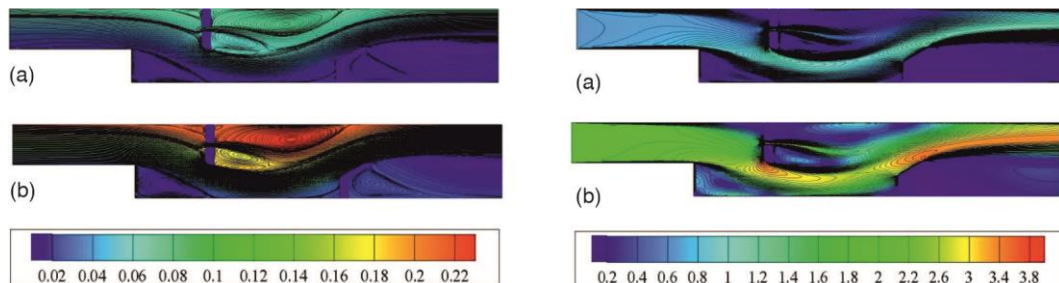


Figure 2. The φ along different Reynolds number; (a) Re = 5000 and (b) Re = 15000

Figure 3. The V fields along different Reynolds numbers

A minority of stream traverses the obstacle hole toward the center of the channel, while the greater part flows downward through the first gap between the top edge of the same

obstacle and the left vertical side of the channel causing a vortex to appear on the left side of the main stream. The flow traverses this perforated obstacle where a split occurs on the upper edge of the same obstacle causing a large vortex to appear on the back along the upper wall of the channel. The presence of the hole in the center of the baffle allowed the large vortex to split into two vortices separated by the secondary current of the hole. Whereas, the main stream goes through the bottom of the channel towards the front side of the second obstacle. The inclined upper side of the latter helped to flow towards the exit by taking parallel lines directly after the same obstacle causing splitting of the stream on the right edge of the obstruction resulting in the appearance of a large cell of circulation as it extends from the inside of the baffle to the end of the stream. In the figure also, the flow maintained its dynamic structure in all cases, but the flow V and the vorticity intensity increased with the increase in Reynolds values.

It is clear that the average velocity field, V , was affected by the presence of the new perforated and tilted baffles, fig. 3. Obviously, all the vortices, whether those below the entrance on the left side of the channel or those visible on the left sides of the baffles, are characterized by a decrease in flow velocity. This regression is due to the current behavior in the opposite direction from the main current. In contrast, all gaps including the pore of the perforated baffle showed gradual increases in velocity causing maximum values of acceleration to appear on the upper left side of the perforated baffle while on the front upper edge of the oblique part of the second obstacle. This flow acceleration is also improved by expanding the range of Reynolds values from 5000-10000.

As for the axial velocity, u , that is, the horizontal component of the velocity, it was characterized by negative and positive values according to its scale, fig. 4. Negative values are characteristic of vortices, *i.e.*, countercurrents, on the right sides of solid surfaces. These vortices have negative currents as they appeared as a result of the separation of the main current at the level of the rear edges of these obstacles. The perforated baffle pore made a different impression by separating the two vortices behind the upper obstacle. While the main currents showed a somewhat rise through the first gap located on the front side of the perforated baffle, while there is a gradual increase in u through the second gap located below the same obstacle. What's more, the main flow accelerates sharply through the third gap above the second obstacle just past the left edge of its top face. Moreover, each of the two models used helped to accelerate the flow, especially in the case of high Reynolds number values.

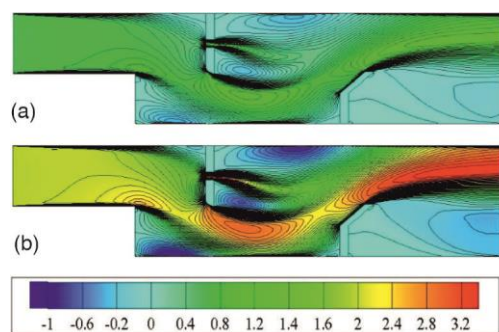


Figure 4. The u fields along different Reynolds numbers; (a) $Re = 5000$ and (b) $Re = 15000$

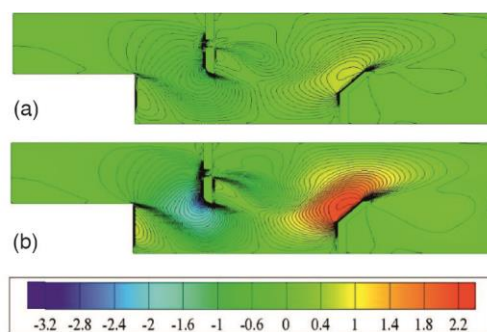


Figure 5. The v fields along different Reynolds numbers

It is also clear from the vertical velocity, v , scale that there are negative values, while others are positive, fig. 5. As is well known, the currents towards the upper sides of the

channel have positive values. For example, the flow through the second obstruction, next to its frontal areas, has positive values. Moreover, the maximum values of v are distributed over the entire left area of the inclined portion of the 2nd baffle especially for currents with improved flow rates such as the case of 15000 of Reynolds number. On the other hand, the currents passing through the 1st obstruction showed negative values in terms of the vertical component of the velocity, especially on the circular surface of the perforated baffle, due to the acceleration of the flow downward, *i.e.*, in the direction opposite to the OY-axis.

Axial velocity, u , curves are evaluated at various sensitive channel stations. For example, fig. 6 shows the evolution of flow acceleration between the inlet and the front of the perforated baffle, exactly on the transverse axis $x = 0.16$ m, fig. 6(a). The flow accelerates in the upper half of the exchanger towards the perforated obstruction, while the appearance of negative u values in the second half of is evidence of the location of a vortex in the region, *i.e.*, in the corner below the entrance.

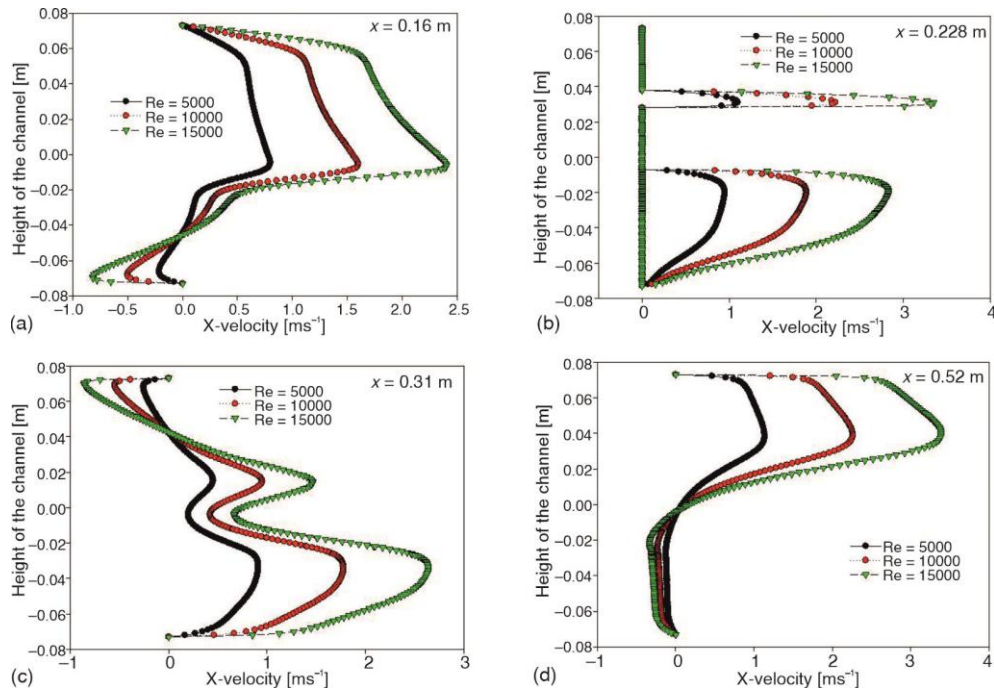


Figure 6. The u profiles along different Reynolds number in various stations; (a) at $x = 0.16$ m, (b) at $x = 0.228$ m, (c) at $x = 0.31$ m, and (d) at $x = 0.52$ m

In the perforated obstruction axle, at its right side, $x = 0.228$ m, the axial velocity values are also analyzed, fig. 6(b). The acceleration of flow through both the pore and the bottom gap is evident. The two flows accelerate from left to right with higher flow rates, where we record large values of axial velocity at the pore level compared to those coming through the gap due to the different flow areas, where the smaller the flow area, the greater the pressure on the flow area, and thus a strong increase in the axial velocity. In the second baffle area, it is clear that the current flow decreases as it approaches the obstacle areas, $x = 0.31$ m on fig. 6(c). The presence of an angled upper section of the obstacle allowed the flow to be directed through the upper gap at strong velocities towards the outlet where the separation of the stream occurred at the level of the leading edge of the same obstacle causing a

large vortex on its back side, $x = 0.52$ m on fig. 6(d). As previously reported in terms of the effect of flow rate on current velocity, the X-velocity improves when the Reynolds number is improved.

By analyzing the dynamic pressure fields, P_d , it is clear that the main flow shows a periodic shape, from left to right, in the presence of clear friction with the hot surface, fig. 7. The improved values of P_d are localized over a large part of the main stream for example across the three gaps and also through the perforated baffle pore. Moreover, the maximum values are shown exactly on the leading edges of the two obstructions. On the contrary, most of the areas, especially those located behind the obstacles, showed a total decrease in P_d , which caused the formation of vortices of different intensities. The field analysis also showed that P_d was affected by different obstruction models. For example, in the first situation, the presence of the pore, helped relieve P_d , on the front area of the upper obstruction. While the second situation, has relieved P_d through the inclination technique applied to its upper part. The influence of P_d values is also indicated by the change in flow rates, where it is clear that there is a direct proportion between the two parameters.

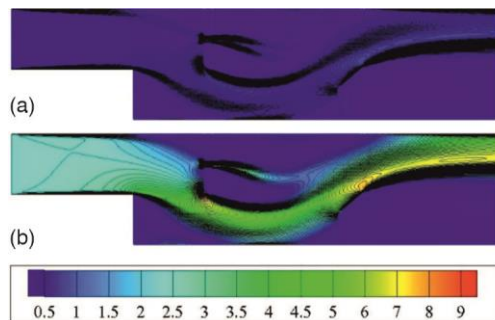


Figure 7. The P fields along different Reynolds number; (a) $Re = 5000$ and (b) $Re = 15000$

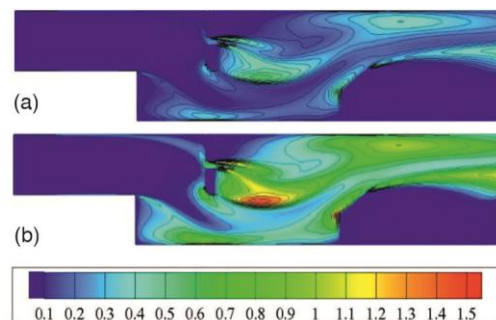


Figure 8. The k fields along different Reynolds number

A significant improvement is evident in both variables, k and μ_t for improved flow rates, that is, in the presence of high Reynolds number, as reported in figs. 8 and 9, respectively. This improvement is evident at the level of the lower vortex of the perforated obstacle, that is, below the secondary stream passing through the pore. This is for the k energy field shown in fig. 8. Whereas, the higher values of μ_t viscosity are evident, behind the inclined obstacle, right next to the upper surface of the exchanger.

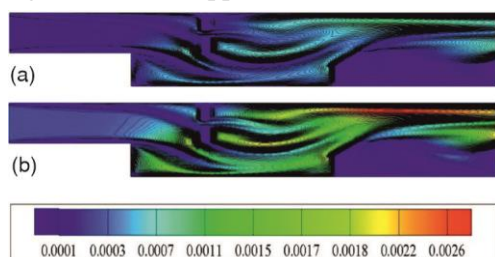


Figure 9. The μ_t fields along different Reynolds number; (a) $Re = 5000$ and (b) $Re = 15000$

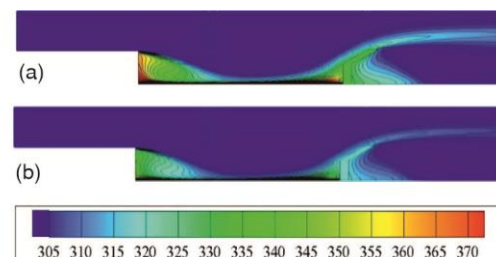


Figure 10. The T fields along different Reynolds number

As shown in the boundary conditions of the studied structure, the lower part of the channel, extending from its left side to the front side of the 2nd obstruction, is subject to a

constant T , $T_w = 375\text{K}$, see fig. 1. It is evident that the thermal field was affected by the presence of inclined baffles and also by those perforated, fig. 10. From the figure, it appears that there is a significant increase in T at both corners behind the left side of the channel and in front of the left side of the 2nd obstruction. These two corners are the centers of two small vortices as a result of the pressure drop in those two areas. While the centering of the upper baffle helped the air flow at high speeds towards the hot area, causing a decrease in the temperature in the region where we record here a very high T gradient.

It is clear from the T curves that there is an appreciable rise in the T values next to the heated space, especially next to the corner below the exchanger entrance where the vortex is located, see $x = 0.16\text{ m}$ on fig. 11(a).

In the middle region of the hot space, there is a decrease in T and this is due to the high V in the region through the bottom gap, see $x = 0.228\text{ m}$ on fig. 11(b). This decrease increases as the flow approaches the 2nd obstruction, see $x = 0.31\text{ m}$ on fig. 11(c). Therefore, there are very high T gradients below the perforated obstacle to the left side of the inclined baffle, which is an enhanced heat transfer in this region, see $x = 0.525\text{ m}$ on fig. 11(d). It is also evident that an inverse relationship between flow rates and fluid T in the exchanger.

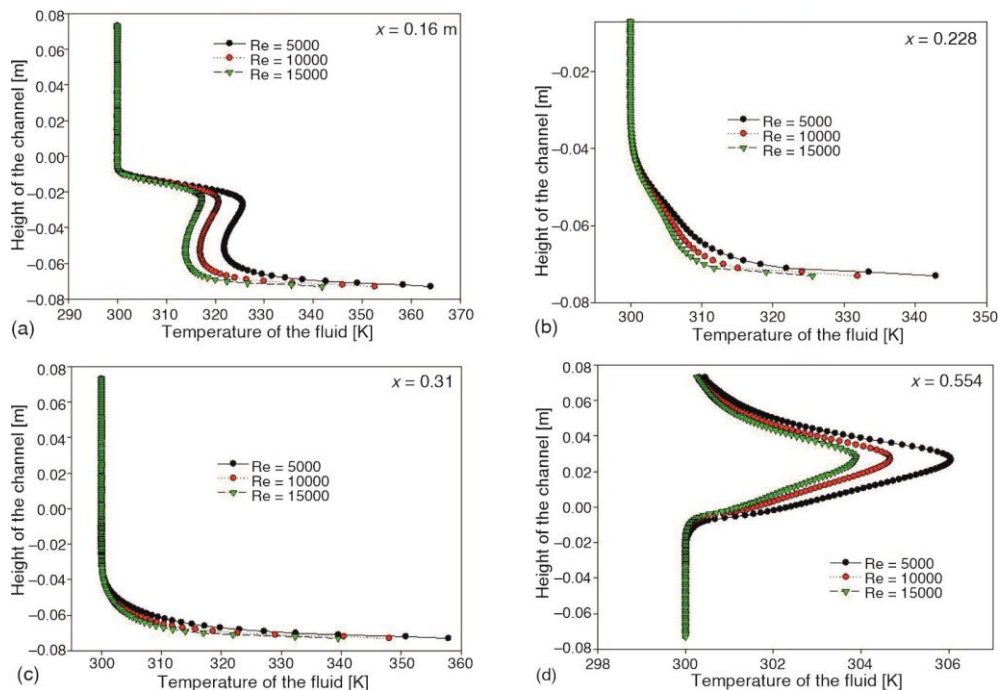


Figure 11. The T profiles along different Reynolds number in various stations; (a) at $x = 0.16\text{ m}$, (b) at $x = 0.228\text{ m}$, (c) at $x = 0.31\text{ m}$, and (d) at $x = 0.554\text{ m}$

Conclusion

The main findings are listed as follows:

- The presence of the pore in the center of the perforated baffle allowed the large vortex to split into two vortices separated by the secondary current of the hole.
- The dynamic pressure showed that its field was affected by different obstacle models. In the 1st situation, the presence of the pore, helped relieve pressure, on the front area of the

upper obstruction. While the 2nd situation, has relieved P_d through the inclination technique applied to its upper part.

- The angled upper side of the inclined baffle helped to flow towards the exit by taking parallel lines directly after the same obstruction causing splitting of the stream on its right edge of the resulting in the appearance of a large cell of recirculation.
- All gaps including the pores showed increases in average velocity causing maximum values of acceleration to appear on the upper left side of the perforated baffle while on the front upper edge of the oblique part of the inclined obstacle.
- In the middle region of the hot space, there is a decrease in temperature, due to the high velocities in the region through the bottom gap. This reduction continues as the flow approaches the inclined obstacle. Therefore, there are very high temperature gradients below the perforated obstacle to the left side of the inclined baffle, which is an enhanced heat transfer in this region.

Finally, it was evident that the use of the three methods, i.e., reconfiguration, perforation and inclination, contributed to the enhancement of the flow structure dynamically, which further enhanced the heat transfer of the heat exchanger.

Acknowledgment

The authors H. Shanak and Jihad Asad would like to thank Palestine Technical University- Kadoorie for supporting this work financially.

References

- [1] Berner, C., et al., Flow Around Baffles, *ASME Journal of Heat Transfer*, 106 (1984), 4, pp. 743-749
- [2] Bazdidi-Tehrani, F., Naderi-Abadi, M., Numerical Analysis of Laminar Heat Transfer in Entrance Region of a Horizontal Channel with Transverse Fins, *Int. Communication in Heat and Mass Transfer*, 31 (2004) 2, pp. 211-220
- [3] Ben Slama, R., Contribution to the Study and the Development of Pumps and Solar Air Collectors, Thesis of Speciality in Energetics, University of Valenciennes, Valenciennes, France, 1987
- [4] Du, B. C., et al., Convective Heat Transfer of Molten Salt in The Shell-and-Tube Heat Exchanger with Segmental Baffles, *Int. Journal of Heat and Mass Transfer*, 113 (2017), Oct., pp. 456-465
- [5] Liu, H. L., et al., Numerical Investigations for Optimizing a Novel Micro-Channel Sink with Perforated Baffles and Perforated Walls, *Int. Communications in Heat and Mass Transfer*, 126 (2021), 105342
- [6] Nakhchi, M. E., et al., Experimental Investigation of Performance Improvement of Double-Pipe Heat Exchangers with Novel Perforated Elliptic Turbulators, *Int. Journal of Thermal Sciences*, 168 (2021), 107057
- [7] Yongsiri, K., et al., Augmented Heat Transfer in a Turbulent Channel Flow with Inclined Detached-Ribs, *Case Studies in Thermal Engineering*, 3 (2014), July, pp. 1-10
- [8] Yan, L., et al., Bubble Behavior of Flow Boiling in Horizontal Rectangular Channels with Inclined Ribs, *Int. Journal of Heat and Mass Transfer*, 75 (2014), Aug., pp. 514-522
- [9] Demartini, L. C., et al., Numeric and Experimental Analysis of the Turbulent Flow Through a Channel with Baffle Plates, *Journal of the Brazilian Society of Mechanical Sciences and Engineering*, 26 (2004), 2, pp. 153-159
- [10] Nasiruddin, M. H., Siddiqui, K., Heat Transfer Augmentation in a Heat Exchanger Tube Using a Baffle, *Int. Journal of Heat and Fluid Flow*, 28 (2007), 2, pp. 318-328
- [11] Menni, Y., et al., Computational Thermal Analysis of Turbulent Forced-Convection Flow in an Air Channel with a Flat Rectangular Fin and Downstream V-Shaped Baffle, *Heat Transfer Research*, 50 (2019), 18, pp. 1781-1818
- [12] Menni, Y., et al., The Solar Air Channels: Comparative Analysis, Introduction of Arc-Shaped Fins to Improve the Thermal Transfer, *J. of Applied and Computational Mechanics*, 5 (2019), 4, pp. 616-626
- [13] Menni, Y., et al., Numerical Analysis of Fluid Flow and Heat Transfer Characteristics of a New Kind of Vortex Generators by Comparison with Those of Traditional Vortex Generators, *Int. Journal of Fluid Mechanics Research*, 47 (2020), 1, pp. 23-42

- [14] Menni, Y., *et al.*, Use of Waisted Triangular-Shaped Baffles to Enhance Heat Transfer in a Constant Temperature-Surfaced Rectangular Channel, *Journal of Engineering Science and Technology*, 12 (2017), 12, pp. 3251-3273
- [15] Menni, Y., *et al.*, Effect of Wall-Mounted V-Baffle Position in a Turbulent Flow Through a Channel: Analysis of Best Configuration for Optimal Heat Transfer, *Int. Journal of Numerical Methods for Heat & Fluid Flow*, 29 (2018), 10, pp. 3908-3937
- [16] Launder, B. E., Spalding, D. B., The Numerical Computation of Turbulent Flow, *Computer Methods in Applied Mechanics and Engineering*, 3 (1974), 2, pp. 269-289
- [17] Patankar, S. V., *Numerical Heat Transfer and Fluid Flow*, McGraw-Hill, New York, USA, 1980